Multibody simulation of an osteogenesis imperfecta child model fit over a harmonic dynamic system

Simulación multicuerpo de un modelo de niño con osteogénesis imperfecta mediante un sistema dinámico armónico

Miguel Ángel Martínez Miranda

Jose Luis Torres Ariza*

Christopher René Torres San Miguel

Instituto Politécnico Nacional,
Ciudad de México, México.
*jtorresa1302@alumno.ipn.mx

03

Abstract

This research examines a 2D Harmonic Dynamic System (HDS) proposed to reduce the kinetic energy transferred to a child body in a motor vehicle crash with the purpose of its subsequent implementation for use in children with bone-degenerative diseases such as osteogenesis imperfecta (OI). The 3D model from the HDS was modified into a simplified 2D model that considers the components present in the XY plane such as rails, springs and shock absorbers that damp excessive movements along the X-axis. The 2D multibody numerical analysis was conducted using Working Model® during an interval of 140 ms; the boundary conditions were in accordance with the United Nations Economic Commission for Europe UN Regulation No. 129 for a CRS frontal test evaluation (CRS). The kinetic behavior observed shows a close correlation between the 2D multibody test and the empiric evaluations from the literature. Although the results were satisfactory for the 2D case proposed, the multibody analysis needs to be revised in a 3D multibody test considering a more detailed CRS and HDS as well as components such as seatbelts.

Keywords: bone-degenerative disease, child ATD, CRS, Harmonic Dynamic System, multibody, osteogenesis imperfecta

Resumen

Esta investigación examina un Sistema Dinámico Armónico (HDS) propuesto en dos dimensiones (2D) que reduce la energía cinética transferida al cuerpo de un niño en un accidente automovilístico con la finalidad de implementarlo posteriormente para el uso en niños con enfermedades óseo-degenerativas, como la osteogénesis imperfecta. El modelo 3D del HDS se modifica para convertirlo en un modelo 2D simplificado que considera los componentes presentes en el plano XY, como rieles, muelles y amortiguadores cuya, función es disminuir los excesivos movimientos suscitados a lo largo del eje longitudinal (eje X) durante un accidente automovilístico. El ensayo multicuerpo 2D se realizó empleando el software Working Model® durante un intervalo de 140 ms; las condiciones de frontera del ensayo se ajustaron conforme al reglamento de la Comisión Económica de las Naciones Unidas para Europa UN/ECE R129 para la evaluación de Sistemas de Retención Infantil (SRI). El comportamiento cinético observado muestra una fuerte correlación entre el ensayo 2D multicuerpo y las pruebas realizadas en laboratorio reportadas en la literatura. Aunque los resultados son satisfactorios para el caso 2D propuesto, es necesario revisar el comportamiento en un análisis multicuerpo 3D considerando un diseño más detallado del SRI y del HDS, así como de elementos como el cinturón de seguridad.

Palabras clave: enfermedad óseo-degenerativa, SRI, ATD infantil, Sistema Dinámico Ármónico, multicuerpo, osteogénesis imperfecta.

Introduction

Degenerative bone changes, such as osteogenesis imperfecta (OI) [1], [2], scoliosis [3] chest wall deformities [4], are diseases that weaken bone internal support structure, which in turn causes an increased risk of fracture and breakage. Some factors associated are genetic predisposition, age related calcium deficits and vitamin deficiency [5], [6], [7]. However, treatments are available to help people enjoy a pleasant and fulfilling life: medication and physical or occupational therapy can provide a way to carry out daily activities with less pain and prevent illness or medical complications [8], [9].

A fracture is a discontinuity caused by impact, torsion or traction forces in the bone that exceed its elastic limit. Trauma is the usual cause of fractures in healthy people, but there are also pathological fractures, which occur without substantial trauma in people who suffer from degenerative diseases. In that sense, bone conditions represent a high risk of injury for OI passengers because a correct positioning inside the vehicle according to safety regulations is difficult to reach. Consequently, patients with advanced bone disease are vulnerable to fractures even in low-speed crashes.

In general, children without hip mobility difficulties can travel in an upright seated position on conventional child restraint systems (CRS). However, some children require specially adapted CRS because their body condition puts them at higher risk of injury in the event of a crash. Although the UN/ECE R129 [10] establishes protection standards for children, according to reports of the European Economic Commission, availability of special CRS is extremely limited [11]. A substantial first step for designing these special CRS is to develop a mechanism to decrease the kinetic energy transmitted to the child. Some systems already exist, such as child seat vehicle anchorage systems [12], crush zone equipped CRS [13], seat integrated kinetic CRS [14] and energy-absorbing webbing CRS [15].

The multibody human model is a way to obtain kinematics and data, such as accelerations, deformation and displacements from a dummy during a crash test scenario. Simcenter Madymo™ by Siemens, for example, is a standard software used to improve and analyze occupant and pedestrian safety in a time-efficient manner. In this research, a 2D frontal multibody sled test following the guidelines established by the UN/ECE R129 will be simulated in Working Model®; the aim is to validate the 2D multibody child model against previous tests reported in the literature.

Two multibody 2D child models were created, the first one was modelled using an anthropometric database of a 3-year-old Hybrid III ATD, and the second was

in accordance with the ATD reported by Martínez *et al.* [16]. The objective is to validate a 2D multibody child with osteogenesis imperfecta via kinematics behavior and the injury data measured in the head and the thorax in terms of acceleration. Throughout this research, a detailed structure is shown to achieve the goals. In the Materials and methods section, the boundary conditions are defined for the frontal sled test according to the UNECE R129 regulation. Additionally, child body properties, such as anthropometric dimensions and mass distribution are presented. In the Results section, the data are compared with those gathered by Turchi *et al.* [17]. Based on the results, it is concluded that the 2D multibody simulation is an accurate and time efficient method to evaluate a crash scenario.

Materials and methods

A 2D multibody frontal test is proposed to observe the kinematic behavior of a child with OI and evaluate the head and chest accelerations. The tests consider the following components: a Harmonic Dynamic System (HDS), a CRS, a car seat, a seat belt, a child dummy and a sled platform. The sled platform geometry and the deceleration pulses for the frontal crash test are based on the UN/ECE R129 regulation. The test is performed in Working Model® during a time interval of 140 milliseconds (ms).

Each component was modelled to obtain their CAD representation on SolidWorks®, then a process of drawing the contour of each component and exporting them in *.dwg extension was executed. The components in *.dwg extension were imported into Working Model®.

Child dummy model parameters

Tables 1 and 2 show the Hybrid III 3yo anthropometric dimensions and mass parameters used to create the child ATD in Working Model®.

Table 1.
Hybrid III 3yo anthropometric dimensions to recreate the ATD in Working Model® [18].
Fuente: elaboración propia.

Parameter	Length (mm)
Sitting height	546.1
Shoulder pivot height	314.96
Hip pivot height	39.37

PARAMETER	LENGTH (MM)
Thigh clearance	86.10
Lower arm and hand length	255.02
Shoulder to elbow length	193.04
Buttock to knee length	256.54
Popliteal height	226.06
Buttock popliteal length	225.55
Chest depth	146.05
Stature	950.5
Foot breadth	58.67
Head circumference	508.00
Chest circumference	539.75
Waist circumference	539.75

TABLE 2.

Hybrid III 3yo mass parameters to recreate the dummy in Working Model® [18].

Fuente: elaboración propia.

COMPONENT	MASS (KG)
Head	2.68
Neck	0.74
Clothed torso	6.54
Upper arm	0.42
Forearm and hand	0.47
Thigh	0.96
Calf	0.60
Foot	0.27
Total	15.46

Osteogenesis imperfecta child ATD parameters

A modified child ATD (Figure 1) was constructed to match the anthropometric and biomechanical parameters consistent with an OI patient. Table 3 shows the mass distribution for each child dummy component according to model 1 developed by Martínez *et al.* [16]. An additional data row is presented to show the equivalent commercial dummy parts. The selected mass distribution corresponds to the 'estimated mass' row to reach the total mass ballasted proposed by [16].

FIGURE 1.
Crash dummy modified to represent a child with OI.
Fuente: elaboración propia.
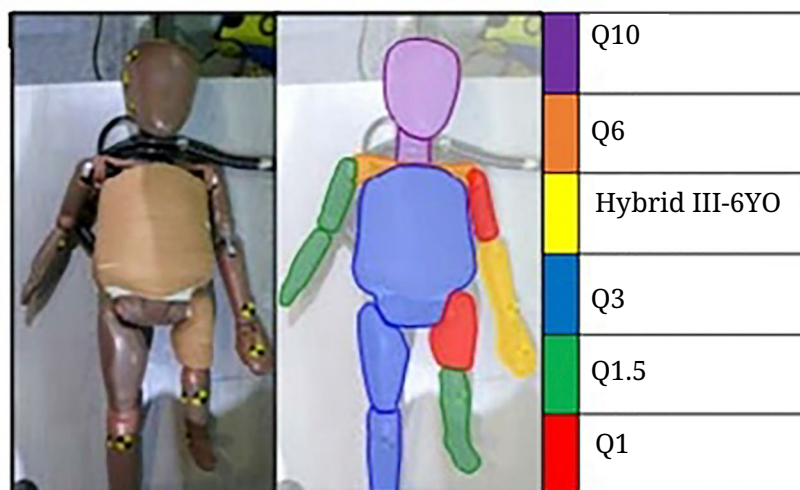
TABLE 3.
Mass distribution for the OI child model [16].
Fuente: elaboración propia.

COMPONENT	ESTIMATED MASS (KG)	UNBALLASTED MASS (KG)	COMMERCIAL DUMMY MODEL
Head	3.86	4.19	Q10
Neck			Q10
Clavicle	11.83	5.80	Q6
Torso			Q3
Right arm	0.37	0.31	Q1.5
Right forearm	0.33	0.23	Q1.5
Left arm	0.41	0.29	Q1
Left forearm	0.20	0.62	HIII 6yo
Right femur	0.97	0.99	Q3
Right tibia	0.57	0.79	Q3
Left femur	1.10	0.50	Q1
Left tibia	0.75	0.46	Q1.5
Total mass	20.39	14.18	
Total mass ballasted		20.96	

Harmonic Dynamic System

The HDS is composed of two main parts: the longitudinal-lateral displacement reduction box (LLDR-b) for movements along the X and Y axes [19], [20], [21], and the anchoring box to keep the CRS fixed. Figure 2a shows the 3D CAD design of the HDS, while 2b shows the LLDR-b schematics.

FIGURE 2.
(a) A view of the HDS 3D model
(b) LLDR-b schematics.

Fuente: elaboración propia.
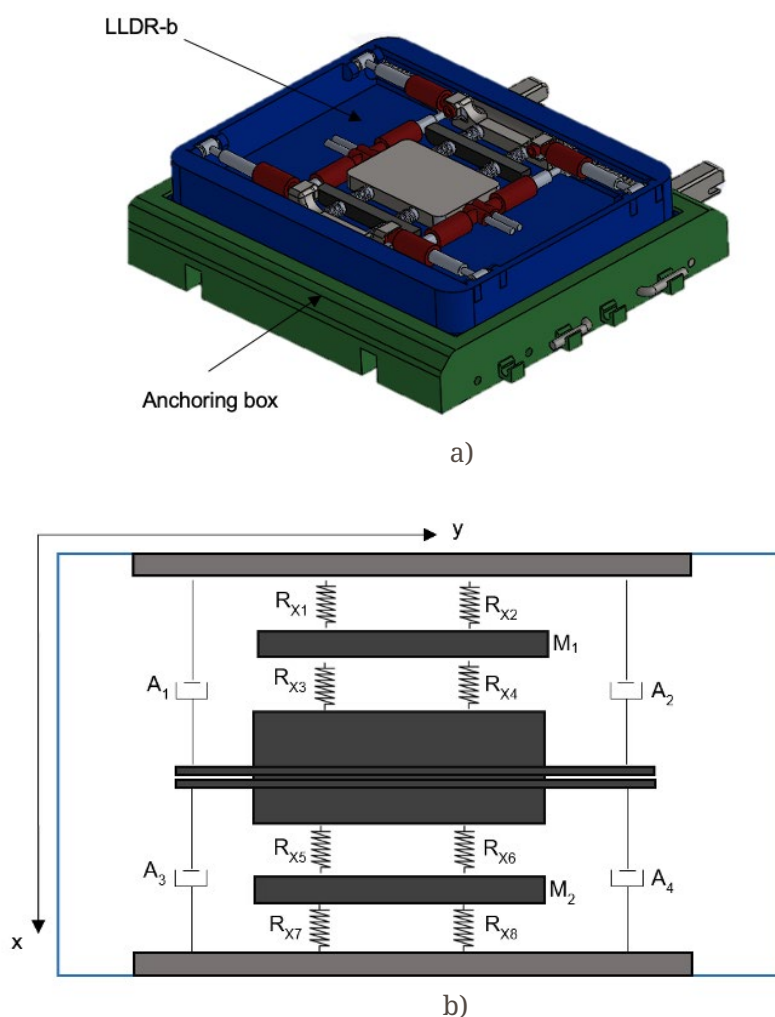
The LLDR-b houses the damping system components. A set of rails allow the linear movement of the slides along the Y-axis, and two transversal rails are located on the main slide to allow displacements along the X-axis; the rails are mounted on the slides with two 2.5 kg mass concentrators, which can also displace along the X-axis. The mass concentrators help reduce the oscillations transmitted to the CRS during a vehicular collision.

The sets of shock absorbers (A_1-A_4) and springs (R_{X1}-R_{X8}) control and damp any abrupt movement of the CRS. The springs are arranged concentrically on the rail, anchored at one end to the LLDR-b surface and at the other end to the dampers The arrange-

ment of one fixed point and one movable point only allows damping longitudinal displacements along the Y-axis. The set of eight springs anchored to the slides and the mass concentrators on the X-axis enables linear displacements in all directions within the XY plane.

According to UN/ECE R129, a CRS must follow the international standard for attachment points for child safety seats denominated as "ISOFIX", but the international regulations overlook specific needs of children with degenerative diseases. To address this demographic, an interchangeable anchorage system is proposed for a faster adjustment to the requirements of special needs users while preserving compliance with the current child safety regulations.

The first design consideration is that the LLDR-b must be firmly anchored. For this reason, a set of stroke limits is attached to the LLDR-b to clamp the box. To make the anchors interchangeable, an arrangement of L-shaped rods and latches is proposed, which works as follows: the longer part of the rods goes through the suspension box, and the shorter part locks into the latches; this interchangeability allows the ISOFIX to be reoriented faster.

Boundary conditions for validation of the sled tests

Working Model® is a 2D software that reduces mathematical and geometric complexity for the analysis of models without three-dimensional interaction, which means that the multibody simulations must be performed in the sagittal view for the frontal sled test.

Frontal sled test

Figure 3 shows the components of the system in accordance with UN/ECE R129.

FIGURE 3.
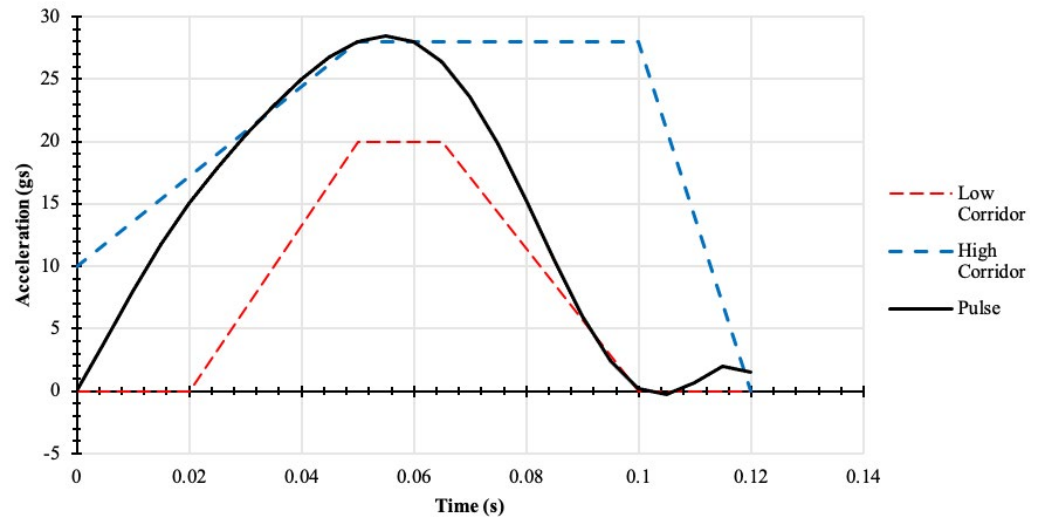Frontal sled test configuration.
Fuente: elaboración propia.
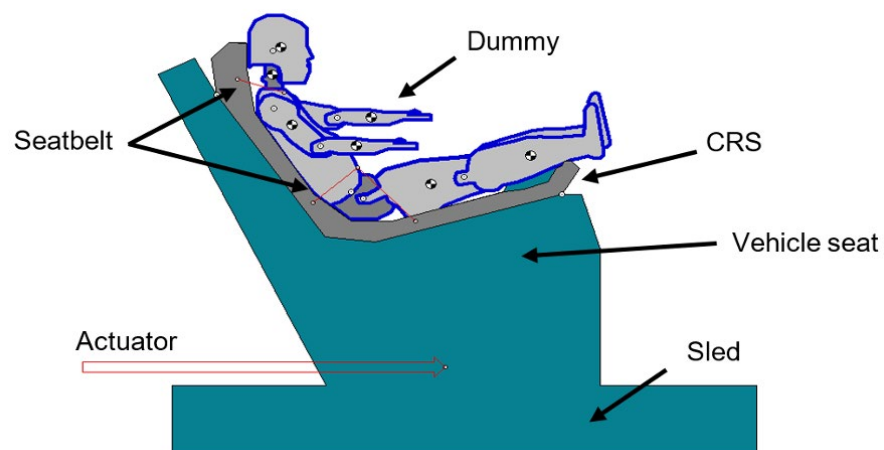
Equation 1 represents the deceleration pulse used for the actuatro $\ddot{x}_{frontal}(t)$; the curve was obtained from a Lagrange interpolation of the sled test data by Kallieris *et al.* [22]. The seatbelt was modeled as a set of 1D elements and assigned with seatbelt material.

$$\ddot{x}_{frontal}(t) = 715.83t + 22493.81t^2 - 1926287.87t^3 + 6.06 \times 10^8 t^5 + 6.86 \times 10^9 t^6 - 1.86 \times 10^{10} t^7 \quad \textbf{(1)}$$

Figure 4 shows that the pulse obtained is located between the UN/ECE R129 corridors for the frontal sled test to evaluate the CRS.

FIGURE 4.
Deceleration pulse vs regulations corridors.
Fuente: elaboración propia.

Boundary conditions to evaluate a child with OI

Considerations for testing are the same as before. In this case, the HDS was included in the evaluation.

Frontal sled test for a child with OI

Figure 5 shows the modified child dummy and the components from the previous validation test (sled platform, actuator, seatbelt and the CRS) in a sagittal view. The same deceleration pulse from Equation 1 was used to evaluate the kinematics behavior.

FIGURE 5.
Frontal sled test to evaluate an OI patient.
Fuente: elaboración propia.
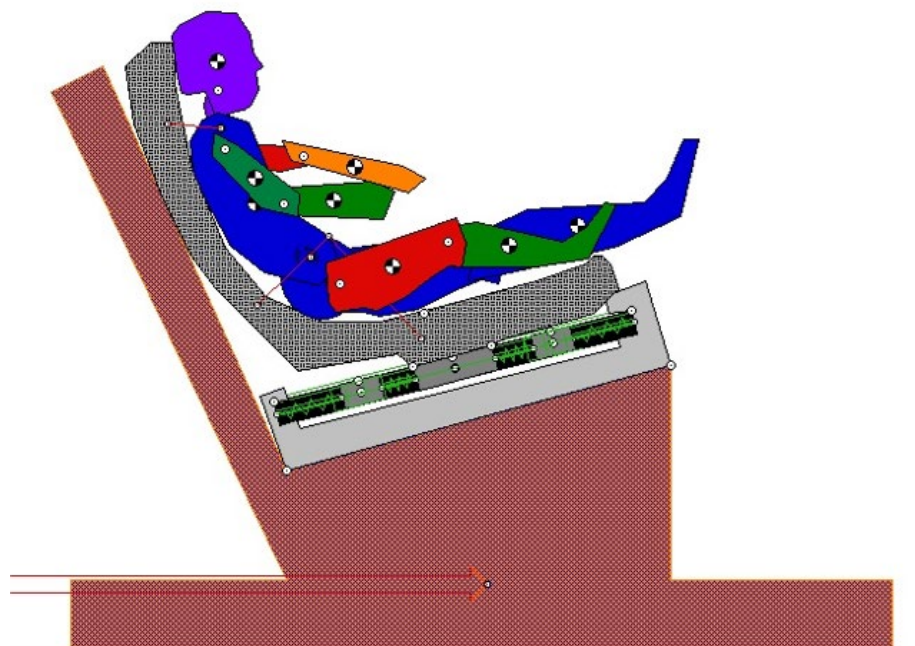
Results and discussion

The kinematics behavior and the head and thorax acceleration from both multibody frontal sled tests (without OI and with OI) are carried out in accordance with the numerical and experimental test by Turchi *et al.* [17]. Each numerical test was performed during a time interval of 140 ms. Additionally, an FIR filter was selected to process the obtained data.

Frontal sled test comparative

Figure 6a shows the deceleration curve for the dummy's head in the X-direction. In the proposed 2D multibody simulation, a maximum force of 31 g is reached at 65 milliseconds. Figure 6b shows the head deceleration curve from the experimental and the numerical tests by Turchi *et al.* [17]. The experimental data by Turchi show a maximum peak of 24 g at 78 ms; whereas for the numerical test 34 g was observed at 59 ms.

FIGURE 6.
Dummy head response curves during the frontal sled test. a) Multibody numerical simulation and b) numerical experimental curves from [17].
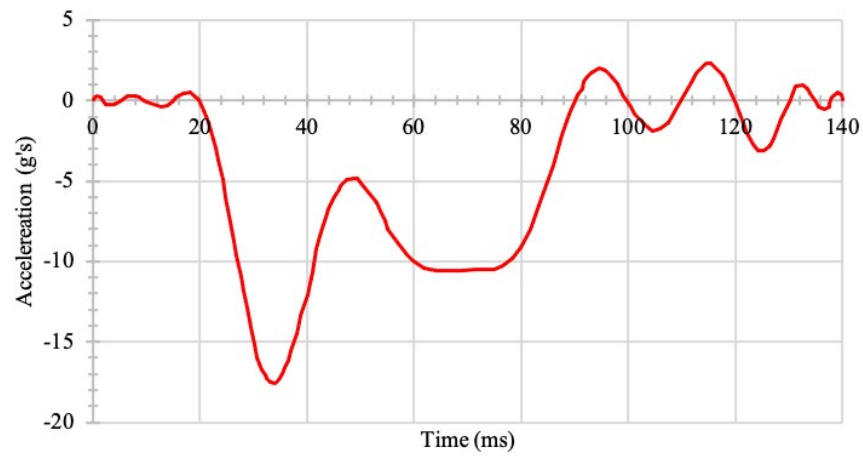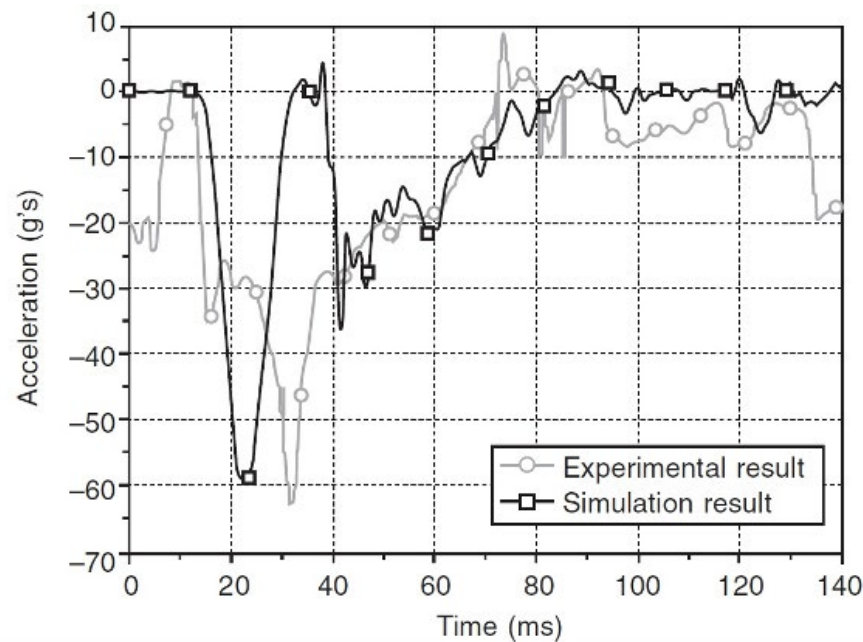Fuente: elaboración propia.
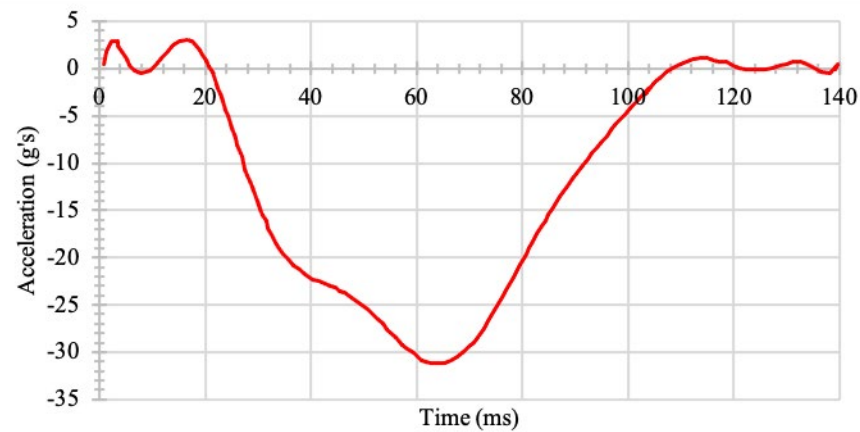
a)

b)

Figure 7 shows the X-axis chest accelerations obtained in the numerical multibody simulation and the data reported in the literature [17]. In the 2D multibody simulation performed, a peak acceleration of –65 g was observed at 30 ms. Data for the simulation test from the literature report a peak of –59 g at 23 ms, and for the experimental test a peak of –62 g at 32 ms. According to the results, the proposed 2D multibody test curve fits better than the numerical test.
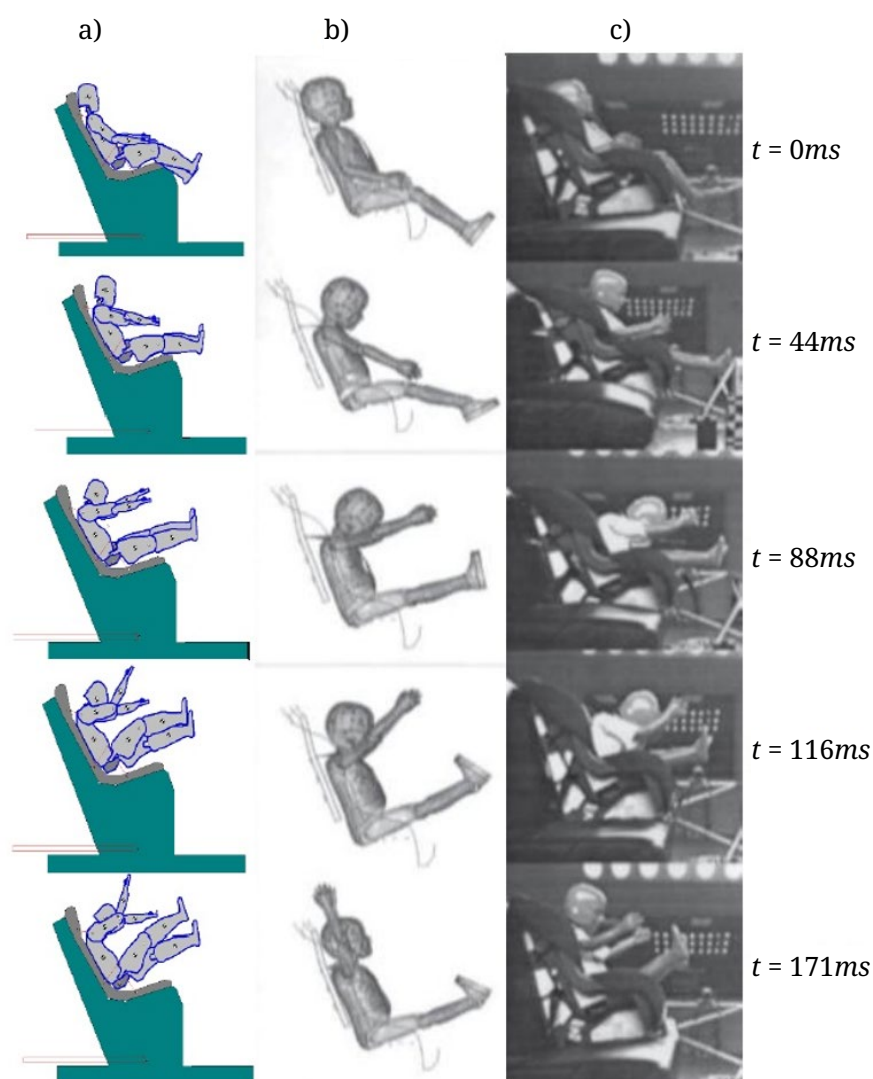
a)

b)

Figure 8 shows the kinematic behavior observed in the 2D numerical multibody simulation and in the tests performed by Turchi *et al.* [17]. Some similarities appear during the interval from 0 to 88 ms in the three models. After that time, the 2D child's multibody shows more significant movement in the upper and lower limbs. The lower limbs suffer a loss of contact with the seat cushion and an offset in the movements of both legs. This biomechanical behavior can represent an increment in the injury severity compared to other body parts, such as the pelvis.

46

Perspectivas de la Ciencia y la Tecnología | Vol. 8 Núm. 15 | julio-diciembre | Facultad de Ingeniería | Universidad Autónoma de Querétaro | ISSN: 2683-3107

a)   b)   c)

$t = 0ms$

$t = 44ms$

$t = 88ms$

$t = 116ms$

$t = 171ms$

Results of the evaluation of an OI patient

The data from the child ATD with OI during the 2D numerical multibody frontal sled test were processed by an FIR filter. The studied interval was 0 to 140 ms.
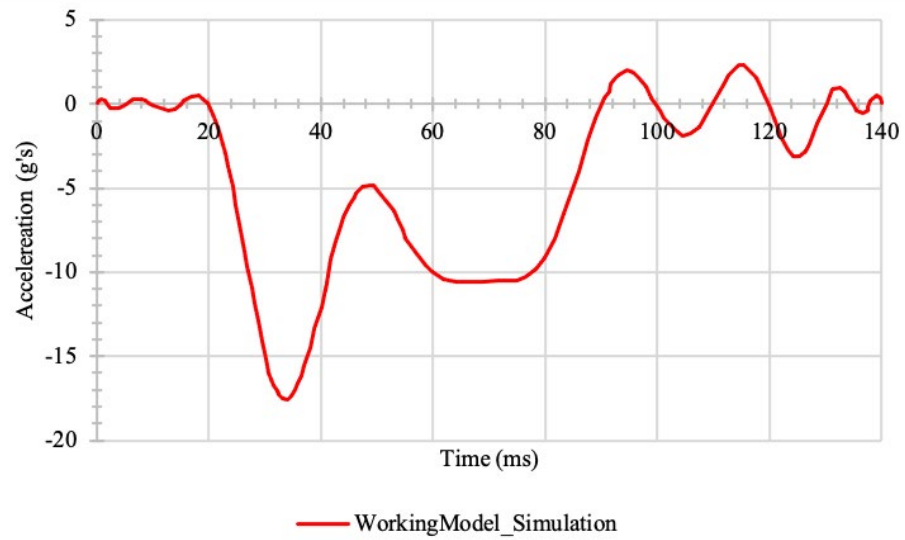
Frontal sled test for a child dummy with OI

Figure 9 shows the deceleration curve for the OI 2D child dummy head on the X-axis as a function of time; a negative peak of 18 g is reached at 35 ms, and a 3 g positive at 115 ms. Figure 10 shows the respective data for the chest region, where two deceleration peaks were observed as a result of the rebound phase.
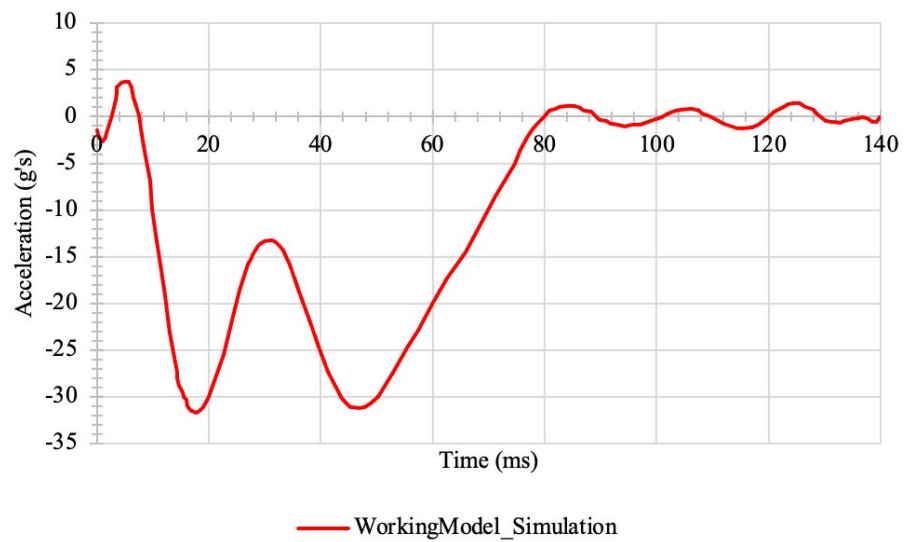
47

Figure 11 shows the kinematic behavior registered in the 2D numerical multibody simulation. During the frontal test, a double rebound behavior is observed at the 20 to 80 ms interval. This behavior is correlated with the multiple peaks illustrated in Figures 9 and 10 for the same interval.
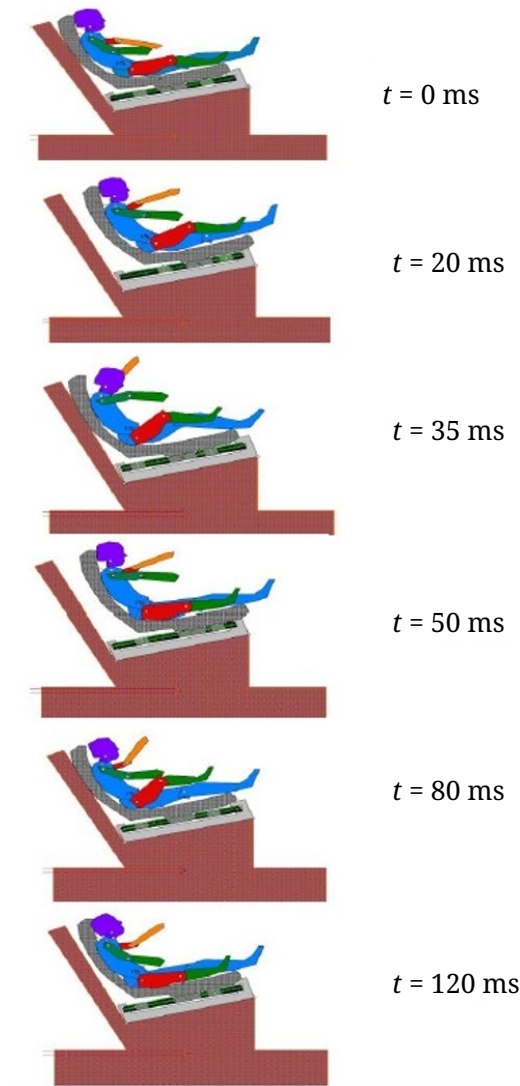
t = 0 ms

t = 20 ms

t = 35 ms

t = 50 ms

t = 80 ms

t = 120 ms

The probability of suffering an injury depends on different factors, such as the CRS employed, vehicle, correct use of the passive safety system, anthropometrics and age. The combination of these components will be reflected in the maximum and minimum peaks suffered in the body parts. In addition, the components discussed in the crash scenario need to be considered. Although the curves from the validation frontal sled test and the experimental are not identical (Figure 8), in general, the behavior is similar. The result could be improved by an optimization process, such as modifying the parameters of dampers and springs.

There are some limitations in this study that could be addressed in future research. Sensitivity analysis is required using different workstations and performance computer configurations to evaluate how the way of processing affects the proposed 2D multibody simulation. Additionally, it is recommended to improve some component properties, such as the geometry of the seatbelt (to avoid oversimplification as a 1D element), and to check that the masses and stiffnesses established for each component are similar to their experimental counterparts.

Conclusions

This research demonstrates the feasibility and effectiveness of using a 2D multibody model in Working Model® to assess a child occupant safety in alignment with the UN/ECE R129 guidelines. The 2D dummy head and thorax replicate closely the kinematic behavior of the 3D dummy model performed in numerical tests and align well with the experimental data from previous sled test research literature.

The deceleration curves obtained from the Harmonic Device System during the frontal sled test show that peak acceleration decreases significantly due to the damping system, which demonstrated an optimal performance for the application of this research work. The result obtained by the 2D child's body when the harmonic mechanism is used cannot be directly contrasted against similar safety mechanisms or conventional CRS since no OI child dummy injury is currently reported in the literature. This absence of research highlights the need to assess injury risk for child with degenerative diseases and future CRS that can accurately protect this specific group. In addition, experimental testing might be the most feasible way to corroborate the results reported by the numerical test evaluated in Working Model®.

Acknowledgments

References

[1] M. Gutiérrez, M. Molina, L. Prieto, J. Parra and A. Bueno, "Osteogénesis imperfecta: nuevas perspectivas," *Revista Española Endocrinología Pediátrica*, vol. 4, suppl. no. 1, 107-118, May 2013, DOI: 10.3266/RevEspEndocrinolPediatr.pre2013.Mar.160

[2] A. Ibáñez and F. Hodgson, "Osteogénesis imperfecta," *Revista Médica Clínica Las Condes*, vol. 32, no. 3, pp. 311-318, May 2021, DOI: 10.1016/j.rmclc.2020.09.004

[3] T. S. Pantoja and L. M. Chamorro, "Escoliosis en niños y adolescentes," *Revista Médica Clínica Las Condes*, vol. 26, no. 1, pp. 99-108, Jan. 2015, DOI: 10.1016/j.rmclc.2015.02.011

[4] A. Wurtz, I. Hysi, L. Benhamed and R. Neviere, "Malformaciones de la pared torácica," *EMC - Aparato Locomotor*, vol. 48, no. 4, pp. 1-13, Dec. 2015, DOI: 10.1016/S1286-935X(15)74984-1

[5] National Institutes of Health (NIH), "Vitamin D: Fact Sheet for Health Professionals." National Institutes of Health. https://ods.od.nih.gov/factsheets/VitaminD-HealthProfessional/

[6] S. Roberts *et al.*, "Ageing in the musculoskeletal system," *Acta Orthopaedica*, vol. 87, no. sup363, pp. 15-25, Dec. 2016, DOI: 10.1080/17453674.2016.1244750

[7]   MedlinePlus, "Aging changes in the bones - muscles - joints." MedLine.gov. https://medlineplus.gov/ency/article/004015.htm

[8]   National Institute of Arthritis and Musculoskeletal and Skin Diseases, "Osteogenesis Imperfecta." NIH.gov. https://www.niams.nih.gov/health-topics/osteogenesis-imperfecta/basics/symptoms-causes

[9]   Sunrise Medical, "Discapacidad física: Las nuevas técnicas de fisioterapia." sunrisemedical.es. https://www.sunrisemedical.es/blog/tecnicas-fisioterapia-discapacidad (accessed Jan. 14, 2024).

[10] *Addendum 128: UN Regulation No. 129*, E/ECE/324/Rev.2/Add.128/Rev.4, United Nations Economic Commission for Europe, 2021.

[11] J. Jiménez. "Viajar con el riesgo de usar el cinturón." *El País*. https://elpais.com/politica/2015/10/06/actualidad/1444128218_442981.html

[12] *Vehicle anchorage system for child seat*, by J. C. Neelis (2004, Mar. 18). Patent US 2004/0051356 A1 [Online]. Available: https://patents.google.com/patent/US6767057B2/en

[13] *Child Seat having a Crush Zone*, by L. C. Strong (2013, Aug. 06). Patent US 8500196 B2 [Online]. Available: https://portal.unifiedpatents.com/patents/patent/US-8500196-B2

[14] *Kinetic Child Restraint Device*, by J. Guenther (2003, Oct. 21). Patent US 6634708 B2 [Online]. Available: https://portal.unifiedpatents.com/patents/patent/US-6634708-B2

[15] *Child restraint device with energy absorbing regions*, by D. Clement (2007, Sep. 13). Patent WO-2007103641-A2 [Online]. Available: https://portal.unifiedpatents.com/patents/patent/WO-2007103641-A2.

[16] L. Martínez, M. de Loma Ossorio, M. Espantaleón, and C. R. Torres, "Estudio antropométrico en sujetos con Osteogénesis Imperfecta para la definición de propiedades de los maniquíes antropomorfos de impacto," in *V Reunión del Capítulo Español de la Sociedad Europea en Biomecánica*, Madrid, Spain, Nov. 2015.

[17] R. Turchi, W. Altenhof, T. Kapoor, and A. Howard, "An investigation into the head and neck injury potential of three-year-old children in forward and rearward facing child safety seats," *International Journal of Crashworthiness*, vol. 9, no. 4, pp. 419-431, Aug. 2004, DOI: 10.1533/ijcr.2004.0300

[18] Humanetics, "Hybrid III Children Series," humaneticsgroup.com. https://www.humaneticsgroup.com/products/anthropomorphic-test-devices/child/hybrid-iii-children-series/3-year-old (accessed, Feb. 22, 2025).

[19] M. Á. Martínez Miranda, C. R. Torres San Miguel and J. A. Flores Campos and L. Martínez Sáez, "Coupling Device for Child Restraint System (CRS) for Infants Affected With Osteogenesis imperfecta: design and numerical assessment," *26th* in *International Technical Conference on the Enhanced Safety of Vehicles (ESV): Enabling a Safer Tomorrow*, Eindhoven, Jun. 2019.

[20] M. Á. Martínez Miranda, C. R. Torres San Miguel, J. A. Flores Campos and M. Ceccarelli, "Numerical Simulation of a 2D Harmonic Oscillator as Coupling System for Child Restraint Systems (CRS)," in *Advances in Italian Mechanism Science*, V. Niola and A. Gasparetto, Ed., Cham: Springer International Publishing, 2021, pp. 492-502.

[21] I. L. Cruz Jaramillo, J. L. Torres Ariza, M. A. Grave Capistrán, E. A. Alcántara Arreola, C. A. Espinoza Garcés, and C. R. Torres San Miguel, "Numerical Dolly Rollover Evaluation Using a Damping-Harmonic System with a Low Back Booster to Reduce Injuries in a Six-Year-Old Child," *Safety*, vol. 10, no. 2, p. 53, Jun. 2024, DOI: 10.3390/safety10020053

[22] D. Kallieris, J. Barz, G. Schmidt, G. Heess, and R. Mattern, "Comparison Between Child Cadavers and Child Dummy by Using Child Restraint Systems in Simulated Collisions," SAE Technical Paper 760815, Jan. 1976, DOI: 10.4271/760815